SUPPORTING INFORMATION

Highly Stable and Strongly Emitting *N*-Heterocyclic Carbene Platinum(II) Biaryl Complexes

Dominik Suter,[a] Luuk T. C. G. van Summeren,[ab] Olivier Blacque,[a] Koushik Venkatesan[ac]*

[a] Department of Chemistry, University of Zurich, Winterthurerstrasse 190, CH-8057, Zurich, Switzerland

[b] Department of Molecular Materials, Radboud University, Nijmegen, 6525 AJ, Netherlands

[c] Department of Molecular Sciences, Macquarie University, NSW 2109, Australia

Table of Contents

Crystal structure determinations

Single-crystal X-ray diffraction data were collected for complexes **3**–**9** at 183(1) K on Rigaku Oxford Diffraction diffractometers[1] associated to an *Oxford Instruments Cryojet XL* cooler using a single wavelength X-ray source (Mo Kα radiation λ = 0.71073 Å, or Cu Kα radiation λ = 1.54184 Å for **4**): the Xcalibur/Ruby area-detector diffractometer for **5**, **8** and **9**, and the SuperNova/Atlas area-detector diffractometer for **3**, **4**, **6** and **7**. The selected single crystals were mounted using polybutene oil on a flexible loop fixed on a goniometer head and immediately transferred to the diffractometer. Pre-experiment, data collection, data reduction and analytical absorption correction[2] were performed with the program suite *CrysAlis^{Pro}*.[3] Using *Olex2*,[4] the structures were solved with *SHELXS*[5] (**3**), SHELXT[6] (**4**, **6**, **7** and **9**) or *Superflip*[7] (**5** and **8**) and refined with *SHELXL*[6] (2017/1) by full-matrix least-squares minimization on F^2. *PLATON*[8] was used to check the result of the X-ray analyses. CCDC numbers 1585222–1585228 contain the supplementary crystallographic data for this paper. These data can be obtained free of charge from The Cambridge Crystallographic Data Centre.

Refinement details and special features

In the crystal structure of **3**, two crystallographically independent molecules are observed in the asymmetric unit. In the molecular structure of **4**, each CF_3 group is disordered over two different sets of positions with site-occupancy ratios of 0.262/0.738(7) and 0.162/0.838(4). The solvent molecules of dimethyl sulfate lie near a two-fold axis and a severe disorder is observed. Many *SHELXL* restraints (*DFIX*, *SADI*, *DANG*, *RIGU*) and constraints (*EADP*) had to be used to correct the geometry of the disordered moieties and the thermal parameters of the corresponding non-H atoms. The site-occupancy factors were sometimes kept fixed according to reasonable thermal parameters. In the crystal structures of **5**–**8**, the metal center is located on a special position (two-fold axis), only one half of the molecule had to be refined, the second half was generated by a symmetry operation. Solvent molecules of chloroform co-crystallized with the main Pt species in the crystal structure of **6** in a ratio 4/1 while in **7** the CF_3 group is disordered over three different sets of positions with site-occupancy factors of 0.178(7), 0.231(7) and 0.591(3). Many *SHELXL* restraints had to be used (*SADI*, *DANG*, *RIGU*, *SUMP*) to treat the disorder, to correct the geometry of the disordered components and the thermal parameters of the corresponding non-H atoms. No special refinement details need to be reported for **9**.

Crystal data for 3 (CCDC-1585228). $C_{20}H_{12}F_8Pt$ (M = 599.39 g/mol): triclinic, space group P-1 (no. 2), a = 7.08664(7) Å, b = 10.86526(11) Å, c = 22.32223(20) Å, α = 88.8330(9)°, β = 85.8093(9)°, γ = 71.7737(11)°, V = 1628.17(3) Å^3, Z = 4, T = 183(1) K, μ(MoKα) = 8.709 mm^{-1}, D_{calc} = 2.445 g/cm^3, 48190 reflections measured (5.4° ≤ 2Θ ≤ 61.0°), 9928 unique (R_{int} = 0.0323, R_{sigma} = 0.0212) which were used in all calculations. The final R_1 was 0.0175 (I > 2σ(I)) and wR_2 was 0.0417 (all data).

Crystal Data for 4 (CCDC-1585227). $C_{32}H_{38}F_6N_4Pt$, 0.4(C_2H_6OS) (M = 819.00 g/mol): monoclinic, space group $I$2/a (no. 15), a = 23.5699(3) Å, b = 13.87832(15) Å, c = 20.6249(2) Å, β = 97.6242(11)°, V = 6686.98(14) Å^3, Z = 8, T = 183(1) K, μ(CuKα) = 8.633 mm^{-1}, D_{calc} = 1.627 g/cm^3, 17466 reflections measured (7.4° ≤ 2Θ ≤ 136.5°), 6027 unique (R_{int} = 0.0324, R_{sigma} = 0.0277) which were used in all calculations. The final R_1 was 0.0411 (I > 2σ(I)) and wR_2 was 0.1078 (all data).

Crystal data for 5 (CCDC-1585224). $C_{38}H_{44}N_4Pt$ (M = 751.86): monoclinic, space group $C$2/c (no. 15), a = 22.1256(7) Å, b = 10.3463(2) Å, c = 14.5683(4) Å, β = 103.657(3)°, V = 3240.66(15) Å^3, Z = 4, T = 183(1) K, μ(MoKα) = 4.362 mm^{-1}, D_{calc} = 1.541 g/cm^3, 30323 reflections measured (5.0° ≤ 2Θ ≤ 61.0°), 4952 unique

(R_{int} = 0.0467, R_{sigma} = 0.0327) which were used in all calculations. The final R_1 was 0.0222 (I > 2σ(I)) and wR_2 was 0.0497 (all data).

Crystal data for 6 (CCDC-1585222). $C_{34}H_{44}Cl_{12}N_4Pt$ (*M* = 1129.22 g/mol): monoclinic, space group *C*2/c (no. 15), *a* = 21.5078(2) Å, *b* = 11.04090(10) Å, *c* = 19.3310(2) Å, *β* = 99.9030(10)°, *V* = 4522.05(8) Å^3, *Z* = 4, *T* = 183(1) K, *μ*(MoKα) = 3.842 mm^{-1}, D_{calc} = 1.659 g/cm^3, 68418 reflections measured (5.7° ≤ 2Θ ≤ 61.0°), 6908 unique (R_{int} = 0.0283, R_{sigma} = 0.0132) which were used in all calculations. The final R_1 was 0.0203 (I > 2σ(I)) and wR_2 was 0.0515 (all data).

Crystal data for 7 (CCDC-1585226). $C_{32}H_{30}F_{14}N_4Pt$ (*M* = 931.69 g/mol): orthorhombic, space group *I*bca (no. 73), *a* = 13.9322(2) Å, *b* = 15.4114(2) Å, *c* = 31.5478(4) Å, *V* = 6773.78(16) Å^3, *Z* = 8, *T* = 183(1) K, *μ*(MoKα) = 4.250 mm^{-1}, D_{calc} = 1.827 g/cm^3, 29186 reflections measured (4.7° ≤ 2Θ ≤ 61.0°), 5159 unique (R_{int} = 0.0245, R_{sigma} = 0.0164) which were used in all calculations. The final R_1 was 0.0200 (I > 2σ(I)) and wR_2 was 0.0475 (all data).

Crystal data for 8 (CCDC-1585225). $C_{38}H_{36}F_8N_4Pt$ (*M* = 895.80): monoclinic, space group *C*2/c (no. 15), *a* = 15.5585(3) Å, *b* = 12.0998(2) Å, *c* = 19.3557(3) Å, *β* = 101.6458(18)°, *V* = 3568.81(11) Å^3, *Z* = 4, *T* = 183(1) K, μ(MoKα) = 4.007 mm^{-1}, *Dcalc* = 1.667 g/cm^3, 42675 reflections measured (5.0° ≤ 2Θ ≤ 61.0°), 5442 unique (R_{int} = 0.0611, R_{sigma} = 0.0271) which were used in all calculations. The final R_1 was 0.0237 (I > 2σ(I)) and wR_2 was 0.0590 (all data).

Crystal data for 9 (CCDC-1585223). $C_{32}H_{34}Cl_6F_8N_4Pt$ (*M* = 1034.42 g/mol): monoclinic, space group $P2_1/n$ (no. 14), *a* = 17.8021(6) Å, *b* = 11.3300(2) Å, *c* = 21.2285(6) Å, *β* = 114.771(4)°, *V* = 3887.8(2) Å^3, *Z* = 4, *T* = 183(1) K, μ(MoKα) = 4.089 mm^{-1}, *Dcalc* = 1.767 g/cm^3, 40030 reflections measured (4.4° ≤ 2Θ ≤ 56.6°), 9556 unique (R_{int} = 0.0366, R_{sigma} = 0.0260) which were used in all calculations. The final R_1 was 0.0320 (I > 2σ(I)) and wR_2 was 0.0861 (all data).

Table S1: Crystal data and structure refinement for **3**–**6**.

Identification code	**3**	**4**	**5**	**6**
Empirical formula	$C_{20}H_{12}F_8Pt$	$C_{32}H_{38}F_6N_4Pt$, $0.4(C_2H_6OS)$	$C_{38}H_{44}N_4Pt$	$C_{30}H_{40}N_4Pt$, $4(CHCl_3)$
Formula weight	599.39	819.00	751.86	1129.22
Temperature/K	183(1)	183(1)	183(1)	183(1)
Crystal system	triclinic	monoclinic	monoclinic	monoclinic
Space group	P-1	I2/a	C2/c	C2/c
a/Å	7.08664(7)	23.5699(3)	22.1256(7)	21.5078(2)
b/Å	10.86526(11)	13.87832(15)	10.3463(2)	11.04090(10)
c/Å	22.32223(20)	20.6249(2)	14.5683(4)	19.3310(2)
α/°	88.8330(9)	90	90	90
β/°	85.8093(9)	97.6242(11)	103.657(3)	99.9030(10)
γ/°	71.7737(11)	90	90	90
Volume/$Å^3$	1628.17(3)	6686.98(14)	3240.66(15)	4522.05(8)
Z	4	8	4	4
$\rho_{calc}g/cm^3$	2.445	1.627	1.541	1.659
μ/mm^{-1}	8.709	8.633	4.362	3.842
F(000)	1128.0	3254.0	1512.0	2232.0
Crystal size/mm^3	0.40 × 0.16 × 0.01	0.16 × 0.04 × 0.03	0.15 × 0.1 × 0.06	0.37 × 0.33 × 0.27
Radiation	MoKα (λ = 0.71073)	CuKα (λ = 1.54184)	MoKα (λ = 0.71073)	MoKα (λ = 0.71073)
2Θ range for data collection/°	5.4 to 61.0	7.4 to 136.5	5.0 to 61.0	5.7 to 61.0
Index ranges	-10 ≤ h ≤ 10, -15 ≤ k ≤ 15, -31 ≤ l ≤ 31	-28 ≤ h ≤ 25, -16 ≤ k ≤ 13, -24 ≤ l ≤ 24	-31 ≤ h ≤ 28, -14 ≤ k ≤ 14, -20 ≤ l ≤ 20	-30 ≤ h ≤ 30, -15 ≤ k ≤ 15, -27 ≤ l ≤ 27
Reflections collected	48190	17466	30323	68418
Independent reflections	9928 [R_{int} = 0.0323, R_{sigma} = 0.0212]	6027 [R_{int} = 0.0324, R_{sigma} = 0.0277]	4952 [R_{int} = 0.0467, R_{sigma} = 0.0327]	6908 [R_{int} = 0.0283, R_{sigma} = 0.0132]
Data/restraints/parameters	9928/0/524	6027/163/450	4952/0/199	6908/18/235
Goodness-of-fit on F^2	1.078	1.128	1.056	1.008
Final R indexes [I>=2σ (I)]	R_1 = 0.0175, wR_2 = 0.0408	R_1 = 0.0411, wR_2 = 0.1067	R_1 = 0.0222, wR_2 = 0.0481	R_1 = 0.0203, wR_2 = 0.0510
Final R indexes [all data]	R_1 = 0.0198, wR_2 = 0.0417	R_1 = 0.0426, wR_2 = 0.1078	R_1 = 0.0256, wR_2 = 0.0497	R_1 = 0.0212, wR_2 = 0.0515
Largest diff. peak/hole / e $Å^{-3}$	0.91/-1.04	0.82/-1.04	1.56/-0.64	1.07/-0.99

Table S2: Crystal data and structure refinement for **7**–**9**.

Identification code	**7**	**8**	**9**
Empirical formula	$C_{32}H_{30}F_{14}N_4Pt$	$C_{38}H_{36}F_8N_4Pt$	$C_{30}H_{32}F_8N_4Pt$, $2(CHCl_3)$
Formula weight	931.69	895.80	1034.42
Temperature/K	183(1)	183(1)	183(1)
Crystal system	orthorhombic	monoclinic	monoclinic
Space group	Ibca	C2/c	$P2_1/n$
a/Å	13.9322(2)	15.5585(3)	17.8021(6)
b/Å	15.4114(2)	12.0998(2)	11.3300(2)
c/Å	31.5478(4)	19.3557(3)	21.2285(6)
α/°	90	90	90
β/°	90	101.6458(18)	114.771(4)
γ/°	90	90	90
Volume/$Å^3$	6773.78(16)	3568.81(11)	3887.8(2)
Z	8	4	4
$\rho_{calc}g/cm^3$	1.827	1.667	1.767
μ/mm^{-1}	4.250	4.007	4.089
F(000)	3632.0	1768.0	2024.0
Crystal size/mm^3	0.21 × 0.15 × 0.03	0.32 × 0.22 × 0.17	0.50 × 0.38 × 0.30
Radiation	MoKα (λ = 0.71073)	MoKα (λ = 0.71073)	MoKα (λ = 0.71073)
2Θ range for data collection/°	4.7 to 61.0	5.0 to 61.0	4.4 to 56.6
Index ranges	-19 ≤ h ≤ 16, -21 ≤ k ≤ 21, -44 ≤ l ≤ 45	-22 ≤ h ≤ 22, -17 ≤ k ≤ 17, -27 ≤ l ≤ 27	-23 ≤ h ≤ 23, -15 ≤ k ≤ 15, -28 ≤ l ≤ 28
Reflections collected	29186	42675	40030
Independent reflections	5159 [R_{int} = 0.0245, R_{sigma} = 0.0164]	5442 [R_{int} = 0.0611, R_{sigma} = 0.0271]	9556 [R_{int} = 0.0366, R_{sigma} = 0.0260]
Data/restraints/parameters	5159/94/310	5442/0/235	9556/0/478
Goodness-of-fit on F^2	1.043	1.191	1.031
Final R indexes [I>=2σ (I)]	R_1 = 0.0200, wR_2 = 0.0436	R_1 = 0.0237, wR_2 = 0.0584	R_1 = 0.0320, wR_2 = 0.0827
Final R indexes [all data]	R_1 = 0.0340, wR_2 = 0.0475	R_1 = 0.0251, wR_2 = 0.0590	R_1 = 0.0364, wR_2 = 0.0861
Largest diff. peak/hole / e $Å^{-3}$	1.18/-0.55	2.16/-0.90	1.98/-1.55

Photophysical Properties

Table S3: Photophysical properties of complexes **2**–**9** recorded at 298 K in solution and as solid powder.

complex	Absorption (CH_2Cl_2) λ_{max}/nm (ε/$M^{-1}cm^{-1}$)	Emission (powder) λ_{max}/nm	ϕ_{em}/%
2	230 (24346), 271 (42508), 287 (30969), 310 (12910)	527, 569, 608	11.0
3	229 (18114), 256 (23381), 273 (11955), 308 (7532)	553	50.2
4	233 (32085), 263 (25295), 331 (6672)	489, 526, 559, 567, 607	27.6
5	235 (45531), 265 (28032), 285 (29667), 301 (28487), 334 (11045)	487, 525, 557, 568, 606	31.4
6	232 (32319), 267 (20866), 334 (7221)	489, 526, 561, 569, 608	17.4
7	229 (25313), 248 (23278), 321 (6058)	485, 508, 535	7.8
8	230 (41833), 245 (30620), 280 (27105), 293 (27577), 325 (10759)	505	54.3
9	230 (28019), 251 (22602), 326 (7133)	550	20.6

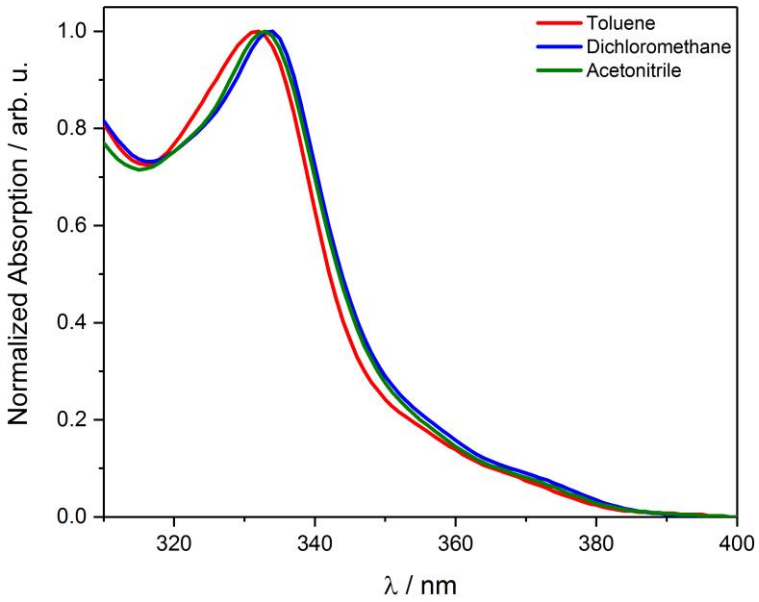

Figure S1: UV/Vis spectra of **6** in different solvents.

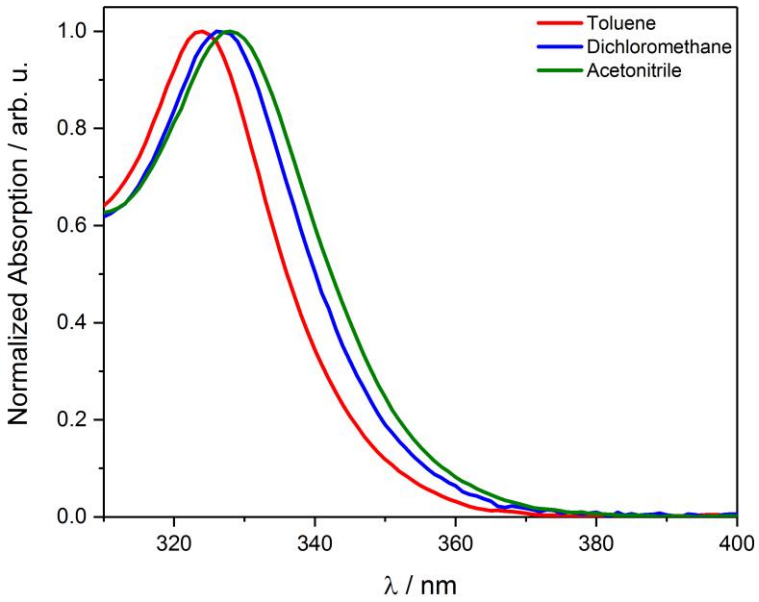

Figure S2: UV/Vis spectra of **9** in different solvents.

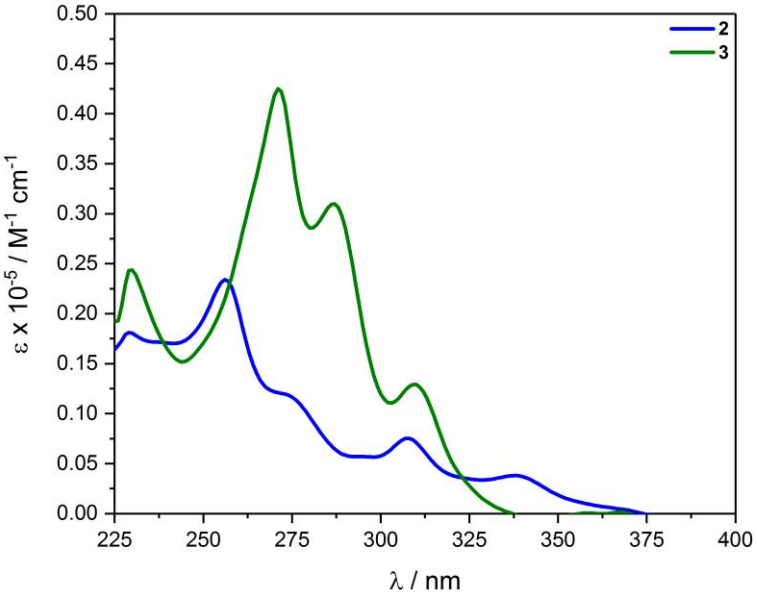

Figure S3: UV/Vis spectra of **2** and **3** recorded in CH_2Cl_2 at room temperature.

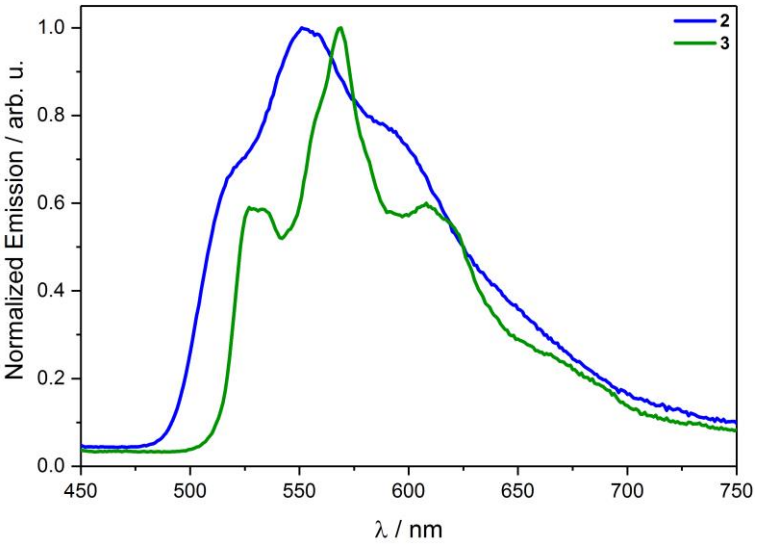

Figure S4: Normailzed emission spectra of complexes **2** and **3** as neat powder recorded at 298 K..

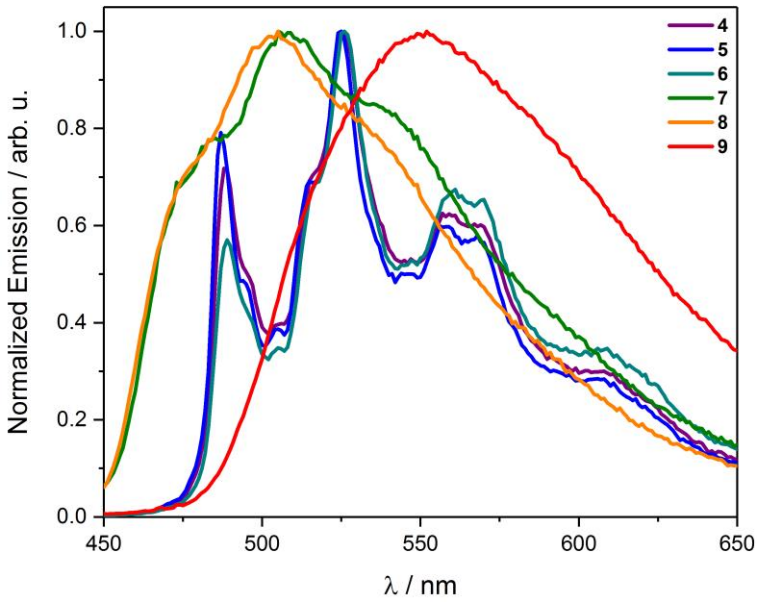

Figure S5: Normalized emission spectra of complexes **4**–**9** as neat powder and recorded at 298 K.

DFT calculations

Computational details

Density functional theory (DFT) and time-dependent DFT (TD-DFT) calculations were used to exemplarily investigate the luminescent properties of the selected compounds **6** and **9**. The calculations were performed with the *Gaussian 09* program package[9] using the hybrid functional PBE1PBE[10] associated with the Stuttgart/Dresden effective core potentials (SDD) basis set[11] for the Pt center augmented with one *f*-polarization function (α = 0.993), with the standard 6-31+G(d) basis set[12] for the remaining atoms, and with the conductive polarizable continuum model (CPCM)[13-14] to take the solvent effects into acount (dichloromethane). The DFT-optimized ground state structures were obtained by restricted DFT calculations while the lowest triplet state structures were obtained by unrestricted DFT calculations (without symmetry restriction). The final geometries were confirmed to be potential energy minima by vibrational frequency calculations at the same level of theory (no imaginary – negative - frequency). On the DFT-optimized ground state S_0 geometry, TD-DFT calculations[15-17] were used to produce the first 25 lowest singlet–singlet and the first 3 singlet–triplet vertical excitations with the corresponding energies, transition coefficients and oscillator strengths. The frontier orbital surfaces and spin density plots were generated by *Gaussview*[18] on *Gaussian 09* formatted checkpoint output files with isovalues set to 0.02 and 0.004, respectively.

TD-DFT results

Selected singlet (S_1, and S_n with oscillator strength $f > 0.1$) and triplet T_m excited states (m = 1-3) calculated with TD-DFT/CPCM (in dichloromethane): vertical excitation energies (nm), transition coefficients ($c > 0.2$), orbitals involved in the transitions, and oscillator strengths f for compounds **6** and **9**.

Compound 6 – singlet excited states

Excited State 1: Singlet-A 3.6437 eV 340.27 nm f=0.0271 <S**2>=0.000

HOMO -> LUMO 0.68950

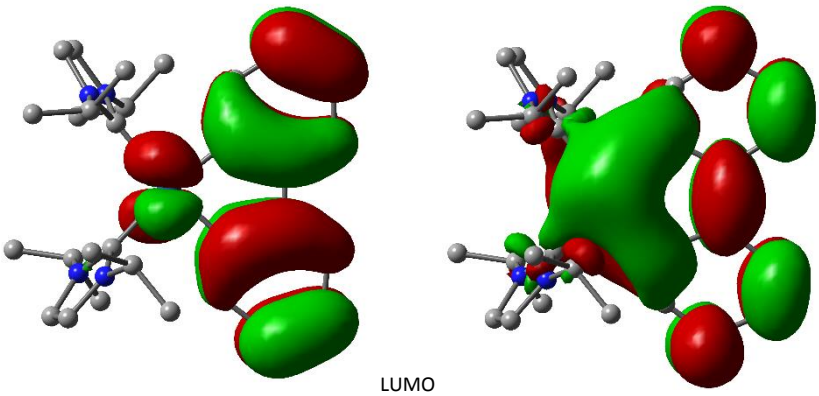

HOMO LUMO

Excited State 2: Singlet-A 4.1418 eV 299.35 nm f=0.0815 <S**2>=0.000

HOMO-4 -> LUMO 0.22563

HOMO -> LUMO+1 0.62066

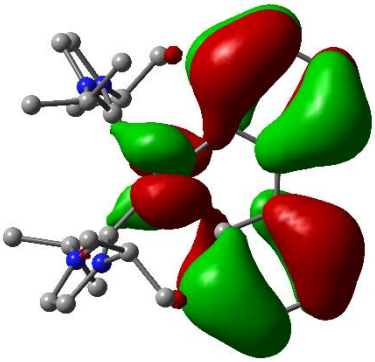

HOMO-4

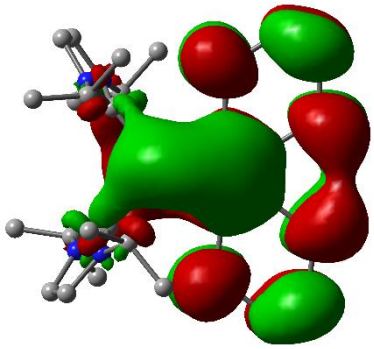

LUMO+1

Excited State 3: Singlet-A 4.1928 eV 295.71 nm f=0.0549 <S**2>=0.000

HOMO-3 -> LUMO 0.22975

HOMO-1 -> LUMO 0.61019

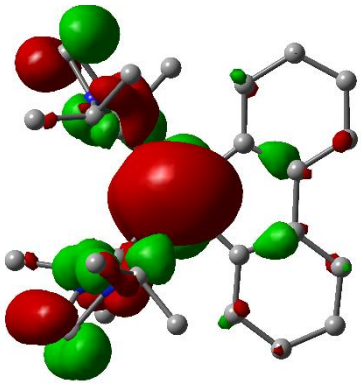

HOMO-3

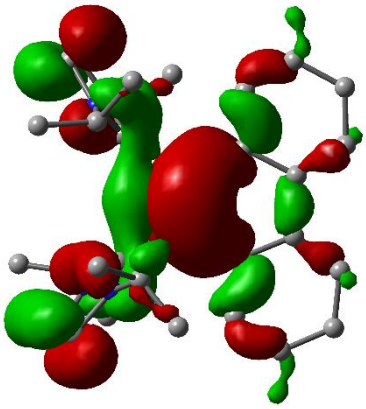

HOMO-1

Excited State 4: Singlet-A 4.2885 eV 289.11 nm f=0.1968 <S**2>=0.000

HOMO-2 -> LUMO 0.68403

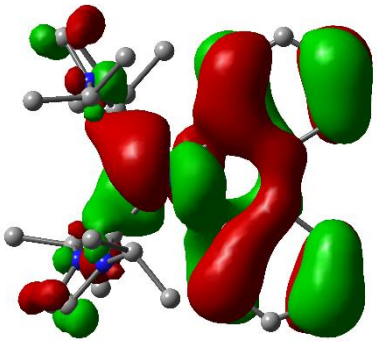

HOMO-2

Excited State 7: Singlet-A 4.7104 eV 263.21 nm f=0.5499 <S**2>=0.000

HOMO-4 -> LUMO 0.60816

Excited State 18: Singlet-A 5.2553 eV 235.92 nm f=0.0589 <S**2>=0.000

HOMO -> LUMO+7 0.39438

HOMO -> LUMO+10 0.23417

Excited State 19: Singlet-A 5.2600 eV 235.71 nm f=0.0799 <S**2>=0.000

HOMO-1 -> LUMO+2 0.57454

HOMO -> LUMO+7 0.26605

Excited State	20:	Singlet-A	5.2705 eV	235.24 nm	f=0.1003	<S**2>=0.000
HOMO-8 -> LUMO		0.19087				
HOMO -> LUMO+14		0.19922				
HOMO -> LUMO+8		0.45471				
HOMO -> LUMO+10		0.20576				
Excited State	23:	Singlet-A	5.4648 eV	226.88 nm	f=0.0637	<S**2>=0.000
HOMO-3 -> LUMO+6		0.28735				
HOMO-1 -> LUMO+6		0.48253				

Compound 6 – triplet excited states

Excited State	1:	Triplet-A	2.6637 eV	465.45 nm	f=0.0000	<S**2>=2.000
HOMO -> LUMO		0.63184				
Excited State	2:	Triplet-A	3.6266 eV	341.88 nm	f=0.0000	<S**2>=2.000
HOMO -> LUMO+1		0.63825				
Excited State	3:	Triplet-A	3.7746 eV	328.47 nm	f=0.0000	<S**2>=2.000
HOMO-3 -> LUMO		0.40051				
HOMO-1 -> LUMO		0.45966				

Compound 9 – singlet excited states

Excited State	1:	Singlet-A	3.7865 eV	327.44 nm	f=0.0141	<S**2>=0.000
HOMO -> LUMO		0.68662				

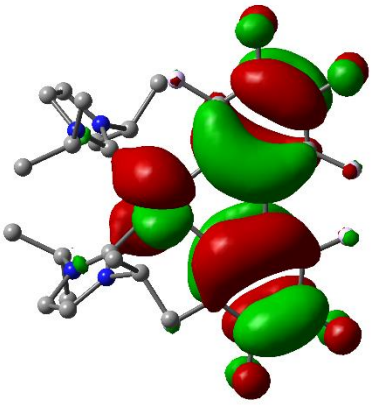

HOMO

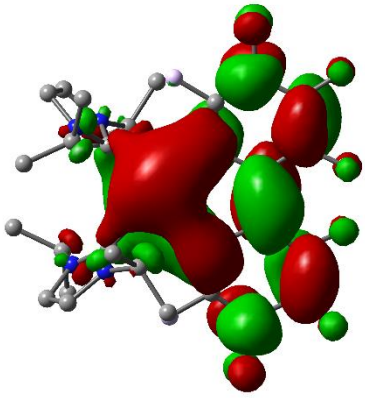

LUMO

Excited State	2:	Singlet-A	4.1103 eV	301.64 nm	f=0.2185	<S**2>=0.000
HOMO-1 -> LUMO		0.68885				

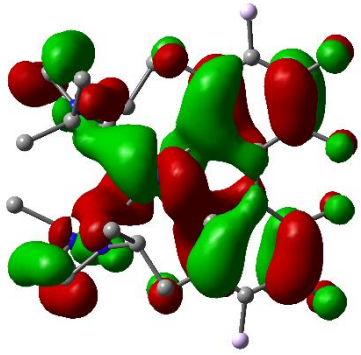

HOMO-1

Excited State 6: Singlet-A 4.6677 eV 265.62 nm f=0.3196 <S**2>=0.000

HOMO-3 -> LUMO 0.26565

HOMO -> LUMO+1 0.43962

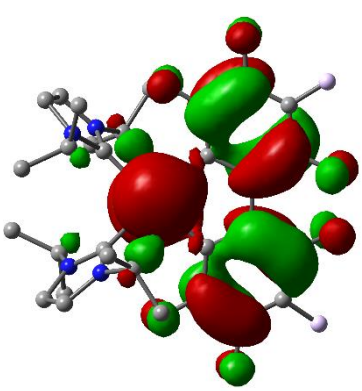

HOMO-3

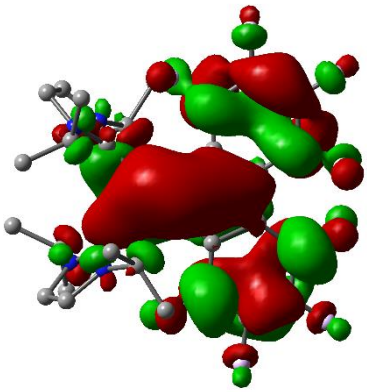

LUMO+1

Excited State 11: Singlet-A 4.9814 eV 248.89 nm f=0.2054 <S**2>=0.000

HOMO-6 -> LUMO 0.31813

HOMO -> LUMO+3 0.54755

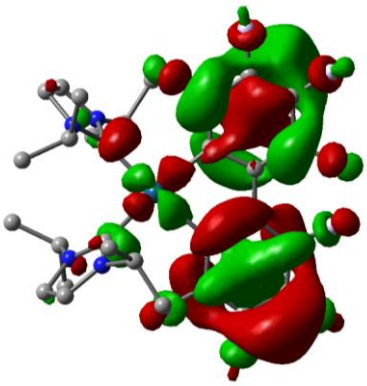

LUMO+3

Excited State 12: Singlet-A 5.0205 eV 246.95 nm f=0.0663 <S**2>=0.000

HOMO-2 -> LUMO+1 0.63983

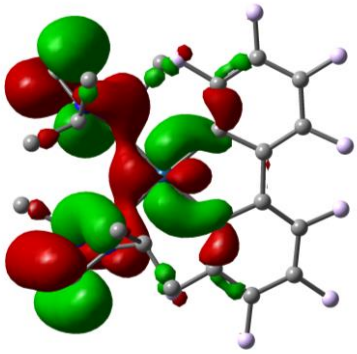

HOMO-2

Excited State 17: Singlet-A 5.4305 eV 228.31 nm f=0.0622 <S**2>=0.000

HOMO-7 -> LUMO 0.33415

HOMO -> LUMO+5 0.40789

Excited State 21: Singlet-A 5.5516 eV 223.33 nm f=0.1530 <S**2>=0.000

HOMO-7 -> LUMO 0.38968

HOMO -> LUMO+8 0.18791

Excited State	25:	Singlet-A	5.6411 eV	219.79 nm	f=0.0743	<S**2>=0.000
	HOMO-4 -> LUMO+2	0.37355				
	HOMO-3 -> LUMO+2	0.27301				
	HOMO -> LUMO+4	0.24916				
	HOMO -> LUMO+5	0.25977				

Compound 9 – triplet excited states

Excited State	1:	Triplet-A	2.7875 eV	444.78 nm	f=0.0000	<S**2>=2.000
	HOMO -> LUMO	0.59965				
Excited State	2:	Triplet-A	3.5436 eV	349.88 nm	f=0.0000	<S**2>=2.000
	HOMO-1 -> LUMO	0.52186				
	HOMO-1 -> LUMO+1	0.19819				
Excited State	3:	Triplet-A	3.6970 eV	335.36 nm	f=0.0000	<S**2>=2.000
	HOMO-3 -> LUMO	0.55478				
	HOMO -> LUMO	0.25496				
	HOMO -> LUMO+1	0.20849				

Cartesian coordinates of the DFT optimized ground-state structure of 6

C	1.55628045	-1.08688843	-0.09183436
C	3.47595791	-2.16064276	0.45340895
C	2.44878718	-0.71771272	2.23075013
H	1.52196774	-0.13381944	2.24602651
C	3.62883296	0.22302950	2.44542900
H	3.63948574	1.01596817	1.69254739
H	4.58229418	-0.31738900	2.40301671
C	1.36235639	-1.88809789	-2.45449729
H	0.40635675	-1.37750042	-2.30660167
C	2.18008097	-1.11794929	-3.48522753
H	2.33432996	-0.08319707	-3.16309774
H	3.15991798	-1.58412751	-3.64399909
C	-1.55842006	-1.08364793	0.09223849
C	-3.18372196	-2.48203778	0.82656628
C	-2.44894630	-0.71436519	-2.23110032
H	-1.52009784	-0.13371182	-2.24697536
C	-2.39990132	-1.80404073	-3.29677423
H	-3.34619784	-2.35567964	-3.34837904
H	-1.59835123	-2.52187183	-3.10047288
C	-1.36739986	-1.88369803	2.45561364
H	-0.41070235	-1.37422407	2.30829454
C	-2.18475681	-1.11249912	3.48584454
H	-3.16528874	-1.57738470	3.64408361
H	-2.33744600	-0.07752875	3.16366575
N	2.00267907	-1.83351545	-1.13831847
N	2.47899184	-1.30949283	0.88767600
N	-2.48093323	-1.30527241	-0.88767149
N	-2.00693633	-1.82848512	1.13908179
Pt	0.00033263	0.27360485	0.00007861
H	1.65226452	-1.10737939	-4.44500242
H	-1.65746269	-1.10265225	4.44591142
H	-2.22679451	-1.35129877	-4.27874109
H	3.55114236	0.68452222	3.43588867
C	3.17833593	-2.48916958	-0.82596441
C	-3.48001690	-2.15385820	-0.45320438
C	-1.29697039	1.83871343	0.28511400
C	-0.71144916	3.13246892	0.18104458
C	-2.64634753	1.79275345	0.67240918
C	-1.46010172	4.28897170	0.42973499
C	0.71779093	3.13097502	-0.18202266
C	-3.39613862	2.94789125	0.92674343
C	-2.80333142	4.20268084	0.79988042
C	1.30072891	1.83601065	-0.28562866
C	1.46872198	4.28590697	-0.43114339
C	2.65000826	1.78725292	-0.67295579
C	2.81177090	4.19683362	-0.80126952
C	3.40207899	2.94081834	-0.92769248
H	-3.70551653	-3.11835672	1.52508121
H	-4.30579850	-2.45555440	-1.07969159
H	3.69848079	-3.12705526	-1.52427669
H	4.30146175	-2.46353990	1.07968423
C	2.39584895	-1.80666477	3.29695839
H	3.34015217	-2.36170600	3.34859277
H	2.22450919	-1.35288809	4.27875008
H	1.59168317	-2.52164611	3.10101817
C	1.11061585	-3.33195710	-2.87214271
H	2.04829432	-3.87960760	-3.02219937
H	0.51643156	-3.86357402	-2.12102546
H	0.56718352	-3.35147264	-3.82242817
C	-1.11771571	-3.32787198	2.87350701
H	-2.05622578	-3.87422166	3.02309150
H	-0.52388666	-3.86031661	2.12269762
H	-0.57477245	-3.34807198	3.82405821
C	-3.62579794	0.23029068	-2.44598494
H	-4.58105972	-0.30687571	-2.40276465
H	-3.63338242	1.02370281	-1.69357072
H	-3.54692709	0.69084955	-3.43678255
H	-3.14422788	0.83045904	0.78395225
H	-4.44054230	2.86413271	1.22369985
H	-3.37561600	5.10740675	0.99417078
H	-0.99902028	5.27188368	0.34824536
H	1.00955961	5.26975176	-0.35007385
H	3.38583969	5.10034953	-0.99592129
H	4.44632293	2.85488178	-1.22459129
H	3.14599872	0.82395105	-0.78419006

Cartesian coordinates of the DFT optimized ground-state structure of 9

C	-1.65231900	-1.41428400	0.40899600
C	-2.86714800	-2.91600600	1.57883300
C	-0.95958000	-1.82590300	2.79600800
H	-0.27941200	-1.01711700	2.50878800
C	-0.14692400	-3.08349600	3.08540800
H	0.45552800	-3.37519300	2.22184600
H	-0.79803900	-3.92340200	3.35572700
C	-2.81933000	-1.63390800	-1.79135700
H	-2.03469100	-0.90413600	-2.01270800
C	-2.59612600	-2.87381500	-2.65013500
H	-1.61448100	-3.31481100	-2.45160400
H	-3.36384800	-3.63440100	-2.46565400
C	-1.65250900	1.41420100	-0.40892800
C	-3.37666600	2.86964500	-0.32458400
C	-0.96015900	1.82585500	-2.79609100
H	-0.28003100	1.01699800	-2.50897000
C	-1.77591900	1.40074100	-4.01194200
H	-2.45392400	2.19710000	-4.34066100
H	-2.37087700	0.50576400	-3.81056500
C	-2.81915500	1.63373800	1.79163000
H	-2.03438400	0.90408600	2.01290200
C	-2.59590300	2.87377900	2.65021300
H	-3.36384800	3.63418700	2.46591400
H	-1.61441800	3.31495100	2.45128600
N	-2.62585600	-1.94366500	-0.37265200
N	-1.81977900	-2.01761300	1.61888500
N	-1.82024100	2.01749400	-1.61881400
N	-2.62605300	1.94338100	0.37284100
Pt	-0.22671300	0.00003000	-0.00003000
H	-2.64613500	-2.60070500	-3.70952700
H	-2.64548200	2.60076300	3.70964800
H	-1.09794900	1.18011200	-4.84285800
H	0.52549900	-2.89628300	3.92932700
C	-3.37630500	-2.86996100	0.32491300
C	-2.86787700	2.91555800	-1.57866100
C	1.35101900	1.32768400	0.05527300
C	2.64511000	0.72607800	0.12908500
C	1.28981900	2.68824500	0.31778600
C	3.74409800	1.48800400	0.52512600
C	2.64513300	-0.72591600	-0.12933000
C	2.40042400	3.46429100	0.63891300
C	3.63393200	2.85513800	0.75649900
C	1.35105600	-1.32754100	-0.05549400
C	3.74412900	-1.48784500	-0.52534300
C	1.28986400	-2.68811200	-0.31794900
C	3.63397600	-2.85499200	-0.75665000
C	2.40047800	-3.46416100	-0.63903600
F	0.11562700	3.36654300	0.30462300
F	2.28069500	4.77987100	0.86933900
F	4.70895500	3.56713100	1.12313500
F	4.95237100	0.95540500	0.78087200
F	4.95239400	-0.95524700	-0.78112000
F	4.70901300	-3.56698700	-1.12324600
F	2.28077200	-4.77975500	-0.86939200
F	0.11566800	-3.36641500	-0.30476200
H	-4.19951500	3.41025700	0.11809700
H	-3.16692000	3.50352400	-2.43310000
H	-4.19913800	-3.41064200	-0.11770800
H	-3.16587600	-3.50405800	2.43332800
C	-1.77517000	-1.40063200	4.01191000
H	-2.45336700	-2.19684100	4.34060200
H	-1.09711900	-1.18019600	4.84280600
H	-2.36992000	-0.50549800	3.81059000
C	-4.18766600	-1.00204000	-2.01853800
H	-4.99458400	-1.69124700	-1.74301000
H	-4.29994800	-0.08397400	-1.43219900
H	-4.31477000	-0.75373300	-3.07743300
C	-4.18735400	1.00173800	2.01922200
H	-4.99443700	1.69077200	1.74375500
H	-4.29964200	0.08354100	1.43308800
H	-4.31418100	0.75363800	3.07820000
C	-0.14752500	3.08345700	-3.08538900
H	-0.79871400	3.92352600	-3.35500400
H	0.45537800	3.37477300	-2.22201100
H	0.52448200	2.89656200	-3.92970500

Electrochemical Studies

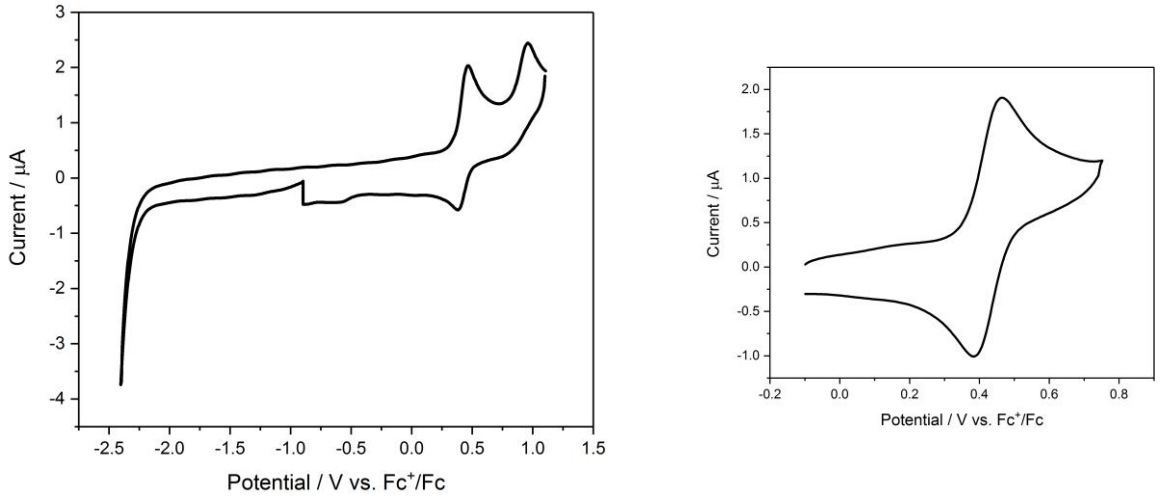

Figure S6: Cyclic voltammogram of **4** in CH_2Cl_2 ([nBu$_4$N][PF_6], 0.1M) at 298 K, glassy carbon electrode, E^0 vs. Fc^+/ Fc with scan rate = 100 mVs^{-1} (left) and separated reversible oxidation (right) event.

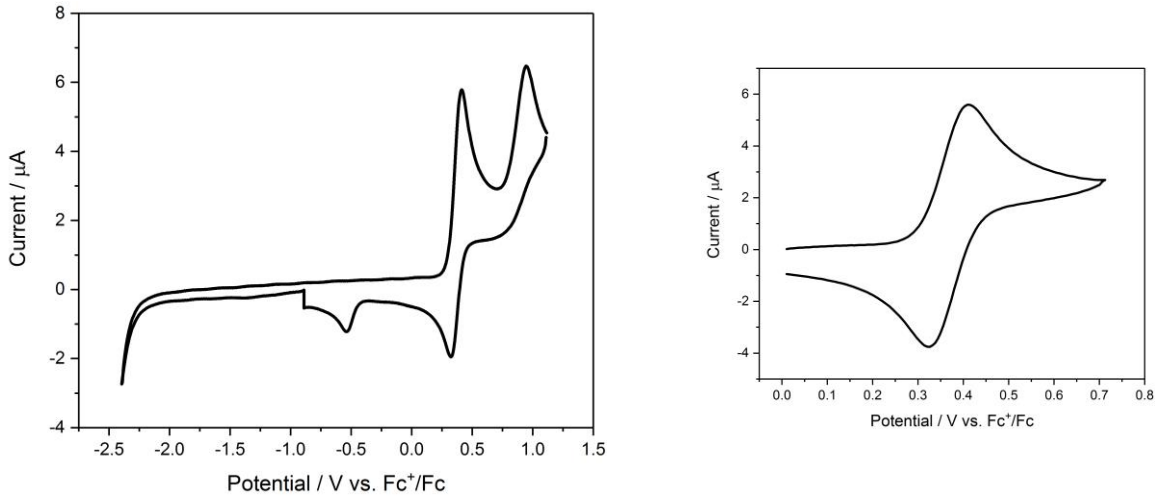

Figure S7: Cyclic voltammogram of **5** in CH_2Cl_2 ([nBu$_4$N][PF_6], 0.1M) at 298 K, glassy carbon electrode, E^0 vs. Fc^+/ Fc with scan rate = 100 mVs^{-1} (left) and separated reversible oxidation (right) event.

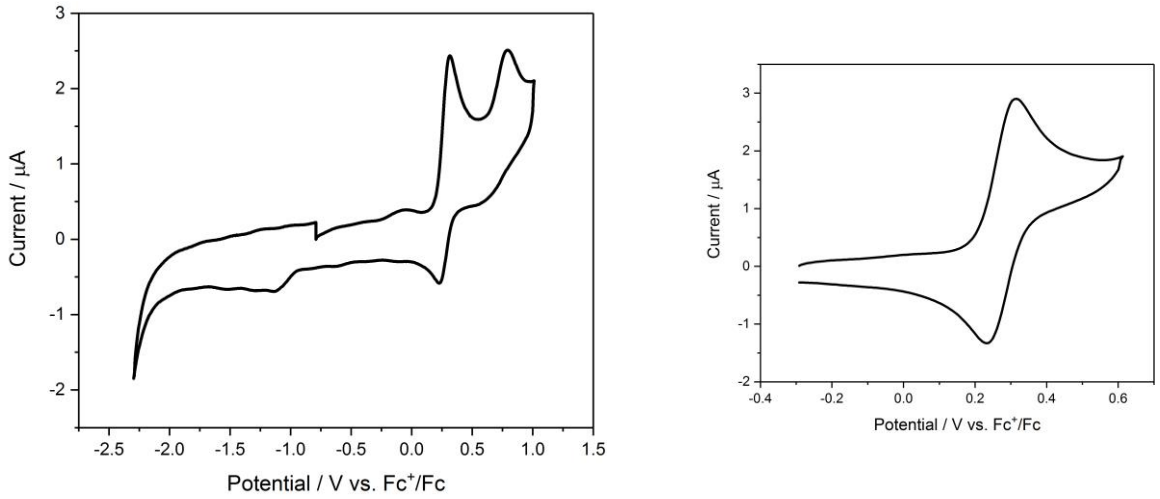

Figure S8: Cyclic voltammogram of **6** in CH_2Cl_2 ([nBu$_4$N][PF_6], 0.1M) at 298 K, glassy carbon electrode, E^0 vs. Fc^+/ Fc with scan rate = 100 mVs^{-1} (left) and separated reversible oxidation (right) event.

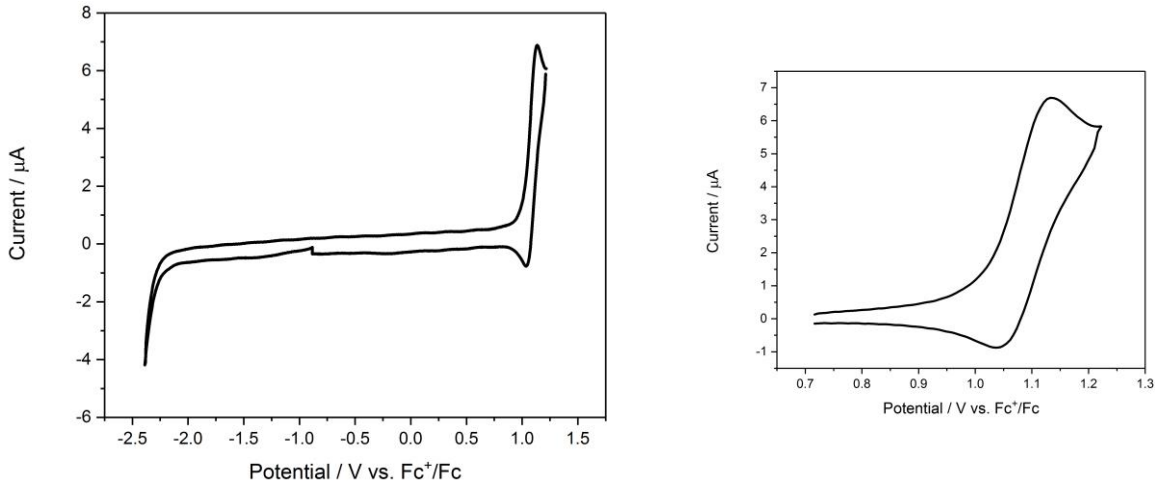

Figure S9: Cyclic voltammogram of **7** in CH_2Cl_2 ([nBu$_4$N][PF_6], 0.1M) at 298 K, glassy carbon electrode, E^0 vs. Fc^+/ Fc with scan rate = 100 mVs^{-1} (left) and separated reversible oxidation (right) event.

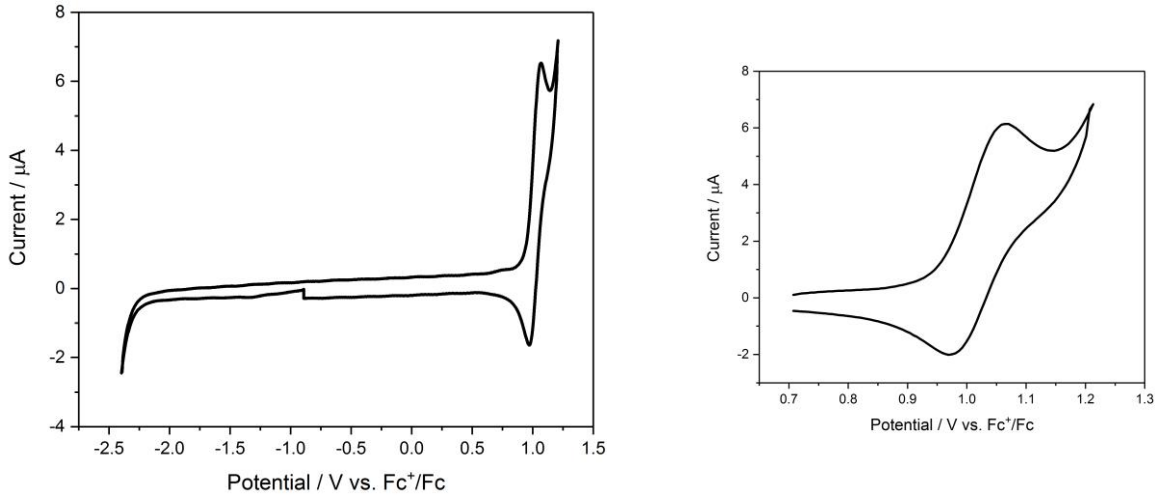

Figure S10: Cyclic voltammogram of **8** in CH_2Cl_2 ([nBu$_4$N][PF_6], 0.1M) at 298 K, glassy carbon electrode, E^0 vs. Fc^+/ Fc with scan rate = 100 mVs^{-1} (left) and separated reversible oxidation (right) event.

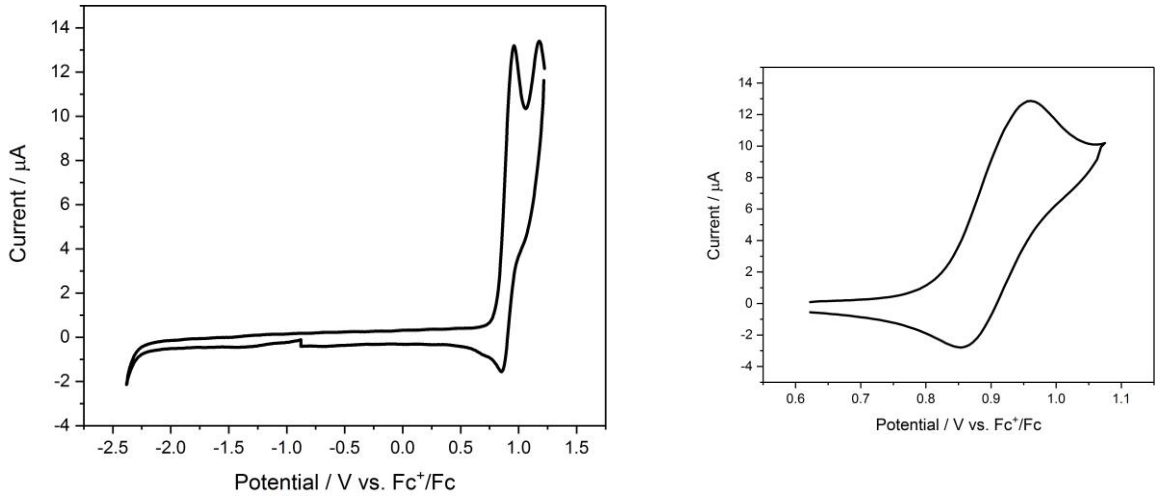

Figure S11: Cyclic voltammogram of **9** in CH_2Cl_2 ([nBu$_4$N][PF_6], 0.1M) at 298 K, glassy carbon electrode, E^0 vs. Fc^+/ Fc with scan rate = 100 mVs^{-1} (left) and separated reversible oxidation (right) event.

Experimental Procedure

General Procedure.[19-20] All manipulations requiring inert atmosphere were carried out using standard Schlenk techniques under N_2 gas. ^{1}H, $^{13}C\{^{1}H\}$, ^{19}F and ^{195}Pt NMR spectra were performed using Bruker 400 MHz and 500 MHz spectrometers. Chemical shifts (δ) are given in parts per million (ppm). Residual proton (^{1}H NMR experiments) and carbon (^{13}C NMR experiments) solvent peaks were used as internal standards referenced to tetramethylsilane (δ 0.00 ppm). Fluorine (^{19}F NMR experiments) spectra were referenced to $CFCl_3$ (δ 0.00 ppm) and platinum (^{195}Pt NMR experiments) spectra were referenced to K_2PtCl_6 in D_2O (δ 0.00 ppm). Coupling constants (*J*) are reported in Hertz (Hz) using the following abbreviations for signal multiplicities: s (singlet); d (doublet); t (triplet); q (quartet); sept (septet); m (multiplet). The assignments were done either with routine 1D or 2D NMR spectroscopies. For TLC analysis, pre-coated Merck Silica Gel60F254 slides were used and visualization was done by luminescence quenching either at 254 nm or 365 nm. Column chromatographic purification (length 15.0 cm: diameter 1.5 cm) of the products was accomplished with silica gel 60, 230–400 mesh. The UV/Vis absorption measurements were performed on a Perkin-Elmer Lambda 35 UV/Vis spectrophotometer. Emission spectra were recorded on an Edinburgh FLS920 spectrometer. As excitation source, a 450 W Xenon lamp was used to excite at the lowest-energy absorption maxima with an excitation slit width of 3–5 nm and emission slit width of 5–10 nm. Absolute quantum yields ϕ_{em} were measured using a F-M01 integrating sphere assembly with doped PMMA thin films at 298 K (estimated uncertainty ± 15 %; with YAG:Ce powder as calibration reference: ϕ_{em} = 97 %). Phosphorescence lifetimes τ in PMMA films were measured with an Edinburgh laser flash photolysis spectrophotometer LP920. As excitation source, a Nd:YAG laser (355 nm) equipped with a single monochromator was used. Cyclic voltammetry measurements were performed with a Methrom 757 VA Computrace using a glassy carbon electrode (d = 2mm) with a Pt counter electrode versus Ag/AgCl reference electrode. Thermo gravimetric analysis (TGA) and differential scanning calorimetry (DSC) were done using a NETZSCHSTA 449C instrument and a sample with known heat of fusion ($RbNO_3$; Δ*H* = 26.6 J/g).

All starting materials were obtained from commercial suppliers and used as received unless otherwise stated. Chemicals that were used are of reagent grade and the solvents for synthesis were of analytical grade.

References

1. Rigaku Oxford Diffraction: 2015.
2. Clark, R. C.; Reid, J. S., The analytical calculation of absorption in multifaceted crystals. *Acta Crystallogr., Sect. A: Found. Crystallogr.* **1995,** *51*, 887-897.
3. *CrysAlis^{Pro}*, CrysAlis^{Pro}, version 1.171.36.20 – 1.171.39.13a; Rigaku Oxford Diffraction: 2015.
4. Dolomanov, O. V.; Bourhis, L. J.; Gildea, R. J.; Howard, J. A. K.; Puschmann, H., OLEX2: a complete structure solution, refinement and analysis program. *J. Appl. Crystallogr.* **2009,** *42*, 339-341.
5. Sheldrick, G. M., A short history of SHELX. *Acta Crystallogr., Sect. A: Found. Crystallogr.* **2008,** *64*, 112-122.
6. Sheldrick, G., SHELXT - Integrated space-group and crystal-structure determination. *Acta Crystallogr., Sect. A: Found. Crystallogr.* **2015,** *71*, 3-8.
7. Palatinus, L.; Chapuis, G., SUPERFLIP - a computer program for the solution of crystal structures by charge flipping in arbitrary dimensions. *J. Appl. Crystallogr.* **2007,** *40*, 786-790.
8. Spek, A., Structure validation in chemical crystallography. *Acta Crystallogr. Sect. D. Biol. Crystallogr.* **2009,** *65*, 148-155.
9. Frisch, M. J.; Trucks, G. W.; Schlegel, H. B.; Scuseria, G. E.; Robb, M. A.; Cheeseman, J. R.; Scalmani, G.; Barone, V.; Mennucci, B.; Petersson, G. A.; Nakatsuji, H.; Caricato, M.; Li, X.; Hratchian, H. P.; Izmaylov, A. F.; Bloino, J.; Zheng, G.; Sonnenberg, J. L.; Hada, M.; Ehara, M.; Toyota, K.; Fukuda, R.; Hasegawa, J.; Ishida, M.; Nakajima, T.; Honda, Y.; Kitao, O.; Nakai, H.; Vreven, T.; Montgomery, J., J. A. ; Peralta, J. E.; Ogliaro, F.; Bearpark, M.; Heyd, J. J.; Brothers, E.; Kudin, K. N.; Staroverov, V. N.; Keith, T.; Kobayashi, R.; Normand, J.; Raghavachari, K.; Rendell, A.; Burant, J. C.; Iyengar, S. S.; Tomasi, J.; Cossi, M.; Rega, N.; Millam, J. M.; Klene, M.; Knox, J. E.; Cross, J. B.; Bakken, V.; Adamo, C.; Jaramillo, J.; Gomperts, R.; Stratmann, R. E.; Yazyev, O.; Austin, A. J.; Cammi, R.; Pomelli, C.; Ochterski, J. W.; Martin, R. L.; Morokuma, K.; Zakrzewski, V. G.; Voth, G. A.; Salvador, P.; Dannenberg, J. J.; Dapprich, S.; Daniels, A. D.; Farkas, O.; Foresman, J. B.; Ortiz, J. V.; Cioslowski, J.; Fox, D. J. Gaussian 09, Revision; Gaussian, Inc.: Wallingford, CT, 2003.
10. Adamo, C.; Barone, V., Toward reliable density functional methods without adjustable parameters: The PBE0 model. *J. Chem. Phys.* **1999,** *110*, 6158-6170.
11. Dunning, J. T. H.; Hay, P. J., *Modern Theoretical Chemistry*. Plenum: New York, 1976; Vol. 3.
12. Ditchfield, R.; Hehre, W. J.; Pople, J. A., Self-Consistent Molecular-Orbital Methods. IX. An Extended Gaussian-Type Basis for Molecular-Orbital Studies of Organic Molecules. *J. Chem. Phys.* **1971,** *54*, 724-728.
13. Barone, V.; Cossi, M., Quantum calculation of molecular energies and energy gradients in solution by a conductor solvent model. *J. Phys. Chem. A* **1998,** *102*, 1995-2001.
14. Cossi, M.; Rega, N.; Scalmani, G.; Barone, V., Energies, structures, and electronic properties of molecules in solution with the C-PCM solvation model. *J. Comput. Chem.* **2003,** *24*, 669-681.
15. Bauernschmitt, R.; Ahlrichs, R., Treatment of electronic excitations within the adiabatic approximation of time dependent density functional theory. *Chem. Phys. Lett.* **1996,** *256*, 454-464.
16. Casida, M. E.; Jamorski, C.; Casida, K. C.; Salahub, D. R., Molecular excitation energies to high-lying bound states from time-dependent density-functional response theory: Characterization and correction of the time-dependent local density approximation ionization threshold. *J. Chem. Phys.* **1998,** *108*, 4439-4449.
17. Stratmann, R. E.; Scuseria, G. E.; Frisch, M. J., An efficient implementation of time-dependent density-functional theory for the calculation of excitation energies of large molecules. *J. Chem. Phys.* **1998,** *109*, 8218-8224.
18. Dennington, R.; Keith, T.; Millam, J. GaussView, Version 5; Semichem Inc.: Shawnee Mission, KS, 2009.
19. Zhang, Y.; Clavadetscher, J.; Bachmann, M.; Blacque, O.; Venkatesan, K., Tuning the Luminescent Properties of Pt(II) Acetylide Complexes through Varying the Electronic Properties of N-Heterocyclic Carbene Ligands. *Inorg. Chem.* **2014,** *53*, 756-771.
20. Bachmann, M.; Suter, D.; Blacque, O.; Venkatesan, K., Tunable and Efficient White Light Phosphorescent Emission Based on Single Component N-Heterocyclic Carbene Platinum(II) Complexes. *Inorg. Chem.* **2016,** *55*, 4733-4745.